ANNALS OF PHYSICS 133, 217–239 (1981)

Two-Dimensional Electron Transport in Semiconductor Layers. I. Phonon Scattering

P. J. PRICE

IBM Thomas J. Watson Research Center, Yorktown Heights, New York 10598

Received July 25, 1980

The basic theory of lattice scattering for electrons in a semiconductor heterolayer, and resulting transport properties in two dimensions parallel to the layer plane, are investigated, specifically for polar semiconductors such as gallium arsenide. Because of polar coupling of the electron states in this system to the lattice modes, the scattering functions are more complicated than is found for the ordinary Bloch states in homogeneous semiconductors. This is true of acoustic modes, as well as optical modes, in that piezoelectric coupling may not be neglected. The ohmic mobility at moderately low temperatures is calculated, and displayed for 150 K. It is a strongly increasing function of the layer thickness. An approximation scheme for higher temperatures is developed. More generally, and particularly for hot electrons, computer calculation of transport properties is necessary. Use of pretabulated and stored functions may be required for this. Monte Carlo simulation will require special procedures, because of the large range of values of the scattering rates and to accommodate the infinities in piezoelectric-coupled scattering. These are developed here.

1. INTRODUCTION

The "heterolayer" semiconductor materials, with alternating layers of differing semiconductors tens to hundreds of angstroms thick, that can be grown by the MBE technique [1] have systems of electron states which differ from the Bloch states from which they derive, and the resulting electronic properties are of interest in several respects: (a) electron motion in the direction normal to the layers (here, the X direction), associated with the formation of "superlattice bands" [2]; (b) phenomena of the energy levels due to quantization of the electron motion in the X direction, for individual layers [3]; (c) transport properties of the two-dimensional systems of itinerant electrons in the "$\perp$" (Y, Z) directions parallel to the layer interfaces [4]. The present paper concerns the theory of the latter transport phenomena, in particular for the "Type I" layer systems, such as GaAs/(Ga, Al) As, in which the active carriers are of one polarity only and layers functioning as barriers for these carriers alternate with layers functioning as "square wells." Dingle *et al.* [4] have reported that, by controlled variation of doping concentration as well as of alloy composition in the MBE process, ionized impurities can be excluded from the GaAs layers and their neighborhood so effectively that the two-dimensional (YZ) mobility is greatly enhan-

0003-4916/81/060217-23$05.00/0

ced—apparently to near the ion-free values, above about 100 K. The limiting mobilities thus obtained invite comparison with the theoretical mobilities calculated by assuming that the scattering between the electron states is only that due to absorption or emission of a lattice phonon. It is assumed below that these phonons are the same (have the same atomic motions) as for the layer semiconductor in bulk (i.e., bulk GaAs in the case of Ref. [4]).

The system to be considered seems to be of considerable physical interest. It is simpler than the analogous inversion layers in a way that allows the transport properties to more directly reflect its essential complexity. The latter introduces relations between electronic structure and properties that are not found in the bulk: (a) the dependence of scattering rates on $a\Delta k_\perp$, where $\Delta k_\perp$ is the change of (YZ) wavevector and a is the layer thickness; (b) the dependence of the scattering on whether the optical-mode quantum $\hbar\omega_0$ is greater or less than E_{12}, the separation of the first and second quantum energy levels; (c) the dependence of scattering and electron transport on κT compared to E_{12} (here κ is the Boltzmann constant).

In the numerical estimates made, below, in terms of bulk semiconductor quantities for the "well" layers, the material assumed is GaAs. The numerical values used, accordingly, for these constants are collected in Table I.

2. Basic Formulas

The "well" electron wave function in a GaAs (or similar) layer may be expanded as usual in the Bloch functions $\phi_\mathbf{k}$ for normalization volume V:

$$\psi = \sum_\mathbf{k} C_\mathbf{k}\phi_\mathbf{k} \tag{1}$$

and it is convenient to deal with the corresponding envelope function

$$\Psi = \sum_\mathbf{k} C_\mathbf{k} V^{-1/2} \exp(i\mathbf{k}\cdot\mathbf{r}). \tag{2}$$

TABLE I

m_0/m^*	15
ϵ_0	12.90
ϵ_∞	10.92
T_0	420 K
ρs_l^2	1.40×10^{12} erg/cm^3
ρs_t^2	0.48×10^{12} erg/cm^3
D	7.0 eV
h_{14}	1.2×10^7 V/cm

Note. These values are principally taken from Rode (Ref. [8]) and Zook (Ref. [7]).

Here ψ, the ϕ, and Ψ are normalized in V, with $\sum | C |^2 = 1$. It is appropriate, at least in the GaAs/(Ga, Al) As case, to assume the Bloch states of (1) to be in the range of the parabolic energy function

$$E_B(\mathbf{k}) = (\hbar^2/2m^*)\, k^2. \tag{3}$$

Consequently, $E_B(\mathbf{k}) = E_B(k_\parallel) + E_B(\mathbf{k}_\perp)$, and Ψ is separable into factors:

$$\Psi = F(x)\, A^{-1/2} \exp(i\mathbf{k}_\perp \cdot \mathbf{r}_\perp). \tag{4}$$

Here A is the normalization area for the YZ plane (so that $V = LA$, where L is the corresponding length for the X direction). Then

$$\int | F |^2\, dx = 1. \tag{5}$$

The quantization in the X direction results in energy levels E_n with envelope eigenfunctions F_n ($n = 1, 2,...$), each level being the edge of a two-dimensional continuum given by

$$E = E_n + E_B(k_\perp). \tag{6}$$

In the "square well" case we have *approximately* [5]

$$F_n = (2/a)^{1/2} \sin[n(\pi/a)\, x] \tag{7}$$

and

$$E_n = n^2(\hbar^2/2m^*)(\pi/a)^2. \tag{8}$$

Results are given below both for a general $F_n(x)$ and for (7) in particular.

In scattering by absorption or emission of a phonon of wavevector $\mathbf{q}$, the YZ wavevector $\mathbf{k}_\perp$ must change by $\mathbf{q}_\perp$; but there is no such selection rule for the X direction. Instead, the matrix element depends on

$$I_n(q_\parallel) \equiv \int F_n^2 \exp(iq_\parallel x)\, dx \tag{9}$$

for scattering within the subband given by (6), and on

$$I_{mn}(q_\parallel) \equiv \int F_m F_n \exp(iq_\parallel x)\, dx \tag{10}$$

for interband scattering. Obviously,

$$\begin{aligned} I_n(0) &= 1, \\ I_{mn}(0) &= 0. \end{aligned} \tag{11}$$

Another identity following from the definition (9), which will be used below, is

$$\int_{-\infty}^{\infty} |\, I_n \,|^2 \, dq_{\parallel} = 2\pi \int \Phi_n{}^2 \, dx, \tag{12}$$

where

$$\begin{aligned} \Phi_n &\equiv F_n{}^2, \\ \Phi_{mn} &\equiv F_m F_n \,. \end{aligned} \tag{13}$$

It is convenient to define

$$1/b_n \equiv 2 \int \Phi_n{}^2 \, dx \tag{14}$$

so that

$$\int_{-\infty}^{\infty} |\, I_n \,|^2 \, dq_{\parallel} = \frac{\pi}{b_n} \,. \tag{15}$$

The analogous result for (10) is

$$\begin{aligned} \int_{-\infty}^{\infty} |\, I_{mn} \,|^2 \, dq_{\parallel} &= \int_{-\infty}^{\infty} I_m^* I_n \, dq_{\parallel} = 2\pi \int \Phi_{mn}^2 \, dx \\ &= 2\pi \int \Phi_m \Phi_n \, dx \equiv \frac{\pi}{b_{mn}} \,. \end{aligned} \tag{16}$$

When F_n is given by (7), the integral on the right of (12) and of (14) is equal to $3/2a$, and hence

$$\begin{aligned} b_n &= a/3 \\ \text{and on the same basis} \qquad & \\ b_{mn} &= a/2 \end{aligned} \tag{17}$$

being independent of n in (7). Equation (15) shows that $1/b$ gives an estimate of the q value at which $|\, I \,|^2$ falls off. Corresponding to (7) are the results from (9) and (10):

$$\begin{aligned} I_n(q) &= \frac{\sin(\frac{1}{2}aq)}{\frac{1}{2}aq} \frac{n^2}{n^2 - (aq/2\pi)^2} P, \\ I_{mn}(q) &= \frac{\substack{\sin \\ \cos}(\frac{1}{2}aq)}{\frac{1}{2}aq} \frac{4mn(aq/\pi)^2}{4m^2n^2 - [m^2 + n^2 - (aq/\pi)^2]^2} P, \end{aligned} \tag{18}$$

where the upper sin( ) is for m and n both even or both odd, the lower cos( ) is for one of them even and the other odd; and P is a phase factor, with $|\, P \,| = 1$ and phase angle $\pm\frac{1}{2}aq$.

3. Scattering Rates

For three-dimensional scattering between Bloch states, the appropriate matrix element is

$$M_{12}^{\pm}(\mathbf{q}) = \left(\frac{N(\mathbf{q}) + \frac{1}{2} \pm \frac{1}{2}}{V}\right)^{1/2} \delta_{12}^{\pm}(\mathbf{q})\, C_{\mathbf{q}}\,, \tag{19}$$

where the upper (lower) sign refers to emission (absorption) of a phonon of wave-vector $\mathbf{q}$ and energy $\hbar\omega_{\mathbf{q}}$, the subscripts 1 and 2 refer to the initial and the final electron states, N is the usual phonon occupation probability

$$N = [\exp(\hbar\omega/\kappa T) - 1]^{-1} \tag{20}$$

and

$$\delta_{12}^{\pm} = \delta_{\mathbf{k}_1, \mathbf{k}_2 \pm \mathbf{q}} \tag{21}$$

is the Kronecker function giving the selection rule for $\mathbf{k}$. Because of the latter, summation over phonons (of a given mode) and summation over final Bloch states amount to the same. The scattering function $W(1, 2)$, equal to the transition rate per unit volume of $\mathbf{k}$ space, is then

$$W_{\mathrm{III}}(1, 2) = W_{\mathrm{III}}^{+} + W_{\mathrm{III}}^{-} = \frac{2\pi}{\hbar} \frac{|C|^2}{(2\pi)^3} \Delta(1, 2), \tag{22}$$

where C and N depend on $\pm\mathbf{q} = \mathbf{k}_1 - \mathbf{k}_2$ and

$$\Delta(1, 2) = N\, \delta(E(1) - E(2) + \hbar\omega) + (N + 1)\, \delta(E(1) - E(2) - \hbar\omega). \tag{23}$$

The scattering rate

$$\frac{1}{\tau(1)} = \int W(1, 2)\, d^3\mathbf{k}_2 \tag{24}$$

depends on the three-dimensional density of states

$$\begin{aligned} g_{\mathrm{III}} &= \int \delta(E - E')\, d^3\mathbf{k}' = 4\pi k^2\, dk/dE \\ &= [2\pi(2m^*)^{3/2}/\hbar^3]\, E_{\mathrm{B}}^{1/2} \end{aligned} \tag{25}$$

by (3), and on the coupling constant C for each mode.

The matrix elements for two-dimensional scattering are obtained from (19) by multiplying by $I(q_{\parallel})$, where I is given by (9) or (10), and applying the Kronecker factor (21) to the $\perp$ components only. Accordingly the transition rates, between

discrete Bloch states, in three dimensions should be multiplied by $|I|^2$ and summed over $q_\parallel$. Then the two-dimensional scattering function is given by

$$W_{II}(1,2) = \int |I(q_\parallel)|^2 W_{III}\, dq_\parallel$$
$$= \frac{2\pi}{\hbar}\frac{1}{(2\pi)^3}\int dq_\parallel |I(q_\parallel)|^2 |C|^2 \Delta(1,2). \tag{26}$$

In the usual model of the optical-mode processes, the phonon energy $\hbar\omega$ is independent of wavevector. Then $\Delta(\ ,\ )$ may be taken outside the integral in (26); it is given by (23) with $E(1)$ and $E(2)$ understood to be the two-dimensional energy functions (6). We may express this result by writing

$$C_{II}^2 = \int |C|^2 |I(q_\parallel)|^2\, dq_\parallel \tag{27}$$

for the factor which replaces $|C|^2$, in (22), to give the formula for W_{II}. In the acoustic-mode case, phonon frequency is propos rtional to wavevector in the range of interest, and $N(q)$ in (23) has an infinity which is cancelled in (22) by a zero because $|C|^2$ is proportional to ω. Then

$$W_{III} = \frac{2\pi}{\hbar}\frac{S}{(2\pi)^3}\, 2\delta(E(1) - E(2)), \tag{28}$$

where

$$S = \frac{\kappa T}{\hbar\omega}|C|^2. \tag{29}$$

In place of (27) we have

$$S_{II} = \int S\, |I(q_\parallel)|^2\, dq_\parallel \tag{30}$$

for the two-dimensional case, replacing S in (28). The two-dimensional analog of (24) is just the corresponding integral over $\mathbf{k}_\perp$-space, and the equivalent of (25) is

$$g_{II} = \int \delta(E - E')\, d^2\mathbf{k}'_\perp = 2\pi k_\perp\, dk_\perp/dE = 2\pi m^*/\hbar^2 \tag{31}$$

by (3) and (6), a constant in each subband. Just as for three dimensions, in non-polar electron-lattice coupling the scattering will to a good approximation be isotropic, and the scattering rate and transport coefficients be accordingly given by closed expressions, in terms of the density of states for scattering (31); but for polar coupling the scattering is anisotropic, and in general only approximate closed-formula results can be obtained.

For acoustic-mode scattering [6], in the "spherical parabolic" case (3), we have in three dimensions

$$S = \kappa T D^2/2\rho s_l^2, \tag{32}$$

where D is the dilational deformation potential, ρ the mass density and s_l the longitudinal velocity of sound in the lattice, and hence there is a constant mean free path

$$\begin{aligned} l &= (2\pi)^2 (v/2g_{\mathrm{III}})\, \hbar/S \\ &= (\pi\hbar^4/m^{*2})\, \rho s_l^2/\kappa T D^2. \end{aligned} \tag{33}$$

For the two-dimensional case, since S is independent of q, by (15) and (30) we have

$$S_{\mathrm{II}} = (\pi/b)\, S. \tag{34}$$

Then, by (31) and (32), there is a constant scattering time

$$\tau = 2b(\hbar^3/m^*)\, \rho s_l^2/\kappa T D^2. \tag{35}$$

Comparing (33) and (35),

$$\frac{l_{\mathrm{III}}}{\tau_{\mathrm{II}}} = \frac{\pi}{b}\frac{\hbar}{2m^*}. \tag{36}$$

The factor $\pi\hbar/2m^*$ on the right is equal to 27.3 cm^2/sec for GaAs; for $b = a/3$ and $a = 10^{-6}$ cm, the right-hand side equals 8.2×10^7 cm/sec.

Since only intra-subband scattering is represented in (34)–(36), they refer to the lowest subband, associated with the lowest level E_1 (the subscript "1" on b having been omitted). When T is appropriately small compared to E_{12}/κ, the acoustic-mode-scattering mobility will be just $e\tau/m^*$, where τ is given by (35). The ratio of two- to three-dimensional mobility is therefore

$$\frac{\mu_{\mathrm{II}}}{\mu_{\mathrm{III}}} = \left(\frac{m^*\kappa T}{2\pi}\right)^{1/2}\frac{3b}{\hbar}. \tag{37}$$

At higher temperatures, μ_{II} is decreased by scattering between the subbands for electron energies $E > E_2$. By (16) and (30), the analog of (34), (35), (36) applies for acoustic-mode scattering between each pair of subbands. One can get some insight by considering the idealized model in which (7) and (8) apply up to large values of n: The acoustic-mode scattering rate at energy E, with $E_n < E < E_{n+1}$, is proportional to

$$g_{\mathrm{II}}\left(\frac{\pi}{b_i} + \sum_j \frac{\pi}{b_{ij}}\right) = g_{\mathrm{II}}\left(\frac{3\pi}{a} + (n-1)\frac{2\pi}{a}\right) \tag{38}$$

in the ith subband where $i \leqslant n$. For large values of n, the coefficient of g_{II} above is $\approx(2m^*E_{\mathrm{B}})^{1/2}\, 2/\hbar$, which equals $g_{\mathrm{III}}/g_{\mathrm{II}}$; so the expression (38) $\approx g_{\mathrm{III}}$, and the scattering rate tends to the three-dimensional value. Realistically, we need to include optical-mode scattering and consider one or a few subbands.

Polar optical mode scattering [6] is given by

$$|C_q|^2 = \frac{2\pi e^2\hbar\omega_0}{q^2}\left(\frac{1}{\epsilon_\infty} - \frac{1}{\epsilon_0}\right) \tag{39}$$

in (19), and in (22) for three dimensions, where ω_0 is the optical mode frequency, and ϵ_∞ and ϵ_0 are the dielectric functions at frequencies $\gg\omega_0$ and $\ll\omega_0$. The denominator q^2 is the sum of $\|$ and $\perp$ components squared, so that (27) depends on

$$J_*(Q) \equiv \int_{-\infty}^{\infty} \frac{|I_*(q)|^2}{Q^2+q^2}\,dq, \tag{40}$$

where "*" means "n" or "mn", and where q and $\mathbf{Q}$ stand for $q_\parallel$ and $\pm(\mathbf{k}_1-\mathbf{k}_2)_\perp$ from here on. The two-dimensional scattering function is then

$$W_{II}(1,2) = \frac{e^2\omega_0}{2\pi}\left(\frac{1}{\epsilon_\infty}-\frac{1}{\epsilon_0}\right) J_*(Q_{12})\,\Delta(1,2), \tag{41}$$

where J_* is J_n or J_{mn}, and the $E(1)$ and $E(2)$ in Δ are the functions (6).

Corresponding to (40) is the exact formula

$$J_*(Q) = \frac{\pi}{Q}\iint dx_1\,dx_2\,\Phi_*(x_1)\,\Phi_*(x_2)\exp(-Q\,|\,x_1-x_2\,|) \tag{42}$$

in terms of (13). We will make use of simpler results for two extreme conditions. If Q is small compared to the q values at which I_n falls off to zero, then in (40) $|\,I_n\,|^2$ can be taken outside the integral with argument $q=0$; hence by (11)

$$J_n \approx \pi/Q \qquad [Q \text{ small}]. \tag{43}$$

Similarly,

$$J_{mn}(0) = \frac{2a}{\pi}\frac{m^2+n^2}{(m^2-n^2)^2}$$

for (7) in particular. (This latter result is obtained from (42), by expanding the exponential factor of the integrand: $1-Q\,|\,x_1-x_2\,|+\cdots$.) In the other extreme, Q is large compared with the q values at which $|\,I\,|^2$ falls to zero, and q may be neglected in the denominator of the integrand of (40). Then by (15), and similarly by (16),

$$\begin{aligned} J_n &\approx \pi/b_nQ^2 \\ J_{mn} &\approx \pi/b_{mn}Q^2 \end{aligned} \qquad [Q \text{ large}] \tag{44}$$

Obviously, the right-hand sides of Eqs. (44) and the first of Eqs. (43) are rigorous upper bounds of $J_*(Q)$. From numerical results such as are plotted in Fig. 2, it is evident that the second of Eqs. (43) gives the maximum value of $J_{mn}(Q)$. The interpolation formula

$$J_n \simeq \pi/[Q(1+b_nQ)] \tag{45}$$

is convenient, even if not accurate. (It corresponds to taking $|\,I_n\,|^2$ equal to $1/(1+b_n^2q^2)$.) Figure 1 shows representative curves of $|\,I_n\,|^2$ and $J_n/\pi a$, and Fig. 2 similarly for $|\,I_{mn}\,|^2$ and $J_{mn}/\pi a$.

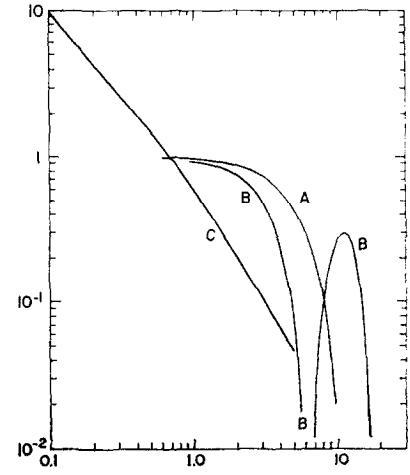

FIG. 1. Intraband scattering functions. Curves A and B are $|I_1|^2$ and $|I_2|^2$, respectively, versus aq. Curve C is $J_1(\pi a)$ versus aQ.

The wavevector change, Q, in general will have a wide range of values in the scattering process. At temperatures small compared to

$$T_0 \equiv \hbar\omega_0/\kappa \tag{46}$$

however, the Q values for intra-subband scattering will be close to the wavevector

$$k_0 = (2m^*\omega_0/\hbar)^{1/2} \tag{47}$$

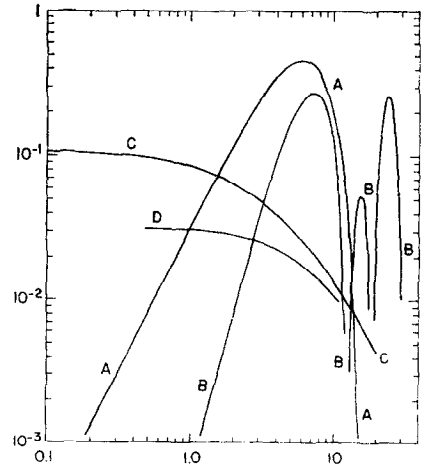

FIG. 2. Interband scattering functions. Curves A and B are $|I_{1,2}|^2$ and $|I_{3,5}|^2$, respectively, versus aq. Curves C and D are $J_{1,2}/(\pi a)$ and $J_{1,3}/(\pi a)$, respectively, versus aQ.

for which $\hbar\omega_0 = E_B(k_0)$. If E_{12} exceeds $\hbar\omega_0$ by several times κT, scattering between subbands will be inappreciable. Then, substantially, the optical-mode scattering will be given by replacing J by $J_1(k_0)$, and Δ by the first term of (23) with N equal to $N_0 = N(\omega_0)$, in (41). The scattering rate will be

$$\frac{1}{\tau} \simeq N_0 J_1(k_0)\, k_0^2 \frac{e^2}{2\hbar}\left(\frac{1}{\epsilon_\infty} - \frac{1}{\epsilon_0}\right). \tag{48}$$

By (8) and (47),

$$\left(\frac{1}{3} ak_0\right)^2 = \frac{\pi^2}{3}\frac{\hbar\omega_0}{E_{12}}. \tag{49}$$

Taking the left-hand side of (49) as $(bQ)^2$, the condition $\hbar\omega_0 < E_{12}$ allows bQ to range from zero to $\pi/\sqrt{3} = 1.814$; the scattering rate will depend on J_1 in (48), a function of ak_0. For GaAs, the value of k_0 is 2.52×10^6 cm^{-1}, so that in practice we are liable to be between the limits (43) and (44). The length $1/k_0$, compared to the layer thickness, has a governing role apart from that of the energies E_n compared to κT and $\hbar\omega_0$.

For sufficiently thin layers (43) will apply and (48) will become

$$\frac{1}{\tau} = k_0 \frac{e^2}{\hbar}\frac{\pi}{2}\left(\frac{1}{\epsilon_\infty} - \frac{1}{\epsilon_0}\right) N_0. \tag{50}$$

For GaAs the coefficient of N_0 on the right of (50) is 1.22×10^{13} sec^{-1}. At $T = 300$ K, we have $N_0 = 0.327$ and $1/\tau = 3.99 \times 10^{12}$ sec^{-1}; at $T = 100$ K, we have $N_0 = 0.0152$ and $1/\tau = 1.85 \times 10^{11}$ sec^{-1}. From (35), the corresponding figures for $1/\tau$, if $a = 0.5 \times 10^{-6}$ cm, are 0.579×10^{12} sec^{-1} and 0.193×10^{12} sec^{-1}. The acoustic-mode rate is greater, at this layer thickness, for temperatures below about 100 K. With increasing thickness the optical-mode rate will decrease more slowly at first, and so will be relatively greater. The acoustic-mode scattering for Eq. (35) is isotropic, and for the situation of Eq. (48) the optical-mode scattering is isotropic, and therefore these τ are the relaxation times proper to the mobility.

In calculating the scattering due to the acoustic-mode phonons, we should consider the piezoelectric coupling as well as the deformation-potential coupling of Eq. (32). It is shown below that the former can become important at temperatures below 100 K, for GaAs, and so might be of interest in the future if not at present. The scattering due to piezoelectric coupling may be calculated separately from the scattering due to deformation coupling, even though for the longitudinal acoustic modes both contribute to each scattering event, because the ratio of the two contributions to the matrix element is imaginary.

Zook [7] has given a detailed account of the piezoelectric scattering in polar semiconductors, including the "zincblende" crystal symmetry that applies to the III–V compounds, and calculated the resulting mobility. His results for the scattering

matrix elements, compared with deformation coupling, are equivalent to the substitution

$$D^2 \to (eh_{14})^2 A/(Q^2 + q^2), \tag{51}$$

where h_{14} is the basic piezoelectric tensor component (see Eqs. (4) and (21) in Ref. [7]), Q and q are the phonon wavevector components as in Eq. (40), and $A(\mathbf{Q}, q)$ is a dimensionless anisotropy factor that depends on the direction of the phonon wavevector in the crystal lattice. For deformation-coupled scattering, the result of (30) is (34), since S is constant in the integral. In the present case, the factor $|I|^2$ of the integrand may be set equal to 1, since the wavevectors Q for (intraband) acoustic-mode scattering are small and the other factor in the integrand will fall off before $|I|^2$ has changed significantly. Then

$$D^2(\pi/b) \to (eh_{14})^2 (\pi/Q) B, \tag{52}$$

where

$$B \equiv \frac{Q}{\pi} \int_{-\infty}^{\infty} \frac{A}{Q^2 + q^2} dq. \tag{53}$$

Both the longitudinal and the two transverse modes contribute, and the constant B has distinct values, B_l and B_t, for these, so that

$$S_{\text{II}} = \frac{\kappa T (eh_{14})^2}{Q} \frac{\pi}{2} \left(\frac{B_l}{\rho s_l^2} + 2 \frac{B_t}{\rho s_t^2} \right). \tag{54}$$

It is assumed in Ref. [7] that the elasticity tensor components are isotropic with respect to the direction, in the crystal, of the axes of their coordinate system. The same approximation is implicit in the separation of the B and s^2 factors in (54) (and similarly in (32), of course). The coefficients A_l, A_t in (51) and (53) nevertheless depend strongly on the direction of the phonon wavevector. By Eq. (23) of Ref. [7],

$$\begin{aligned} A_l &= 36\lambda^2\mu^2\nu^2, \\ A_l + 2A_t &= 4(\lambda^2\mu^2 + \mu^2\nu^2 + \nu^2\lambda^2), \end{aligned} \tag{55}$$

where λ, μ, ν are the direction cosines of the phonon wavevector relative to the three (1, 0, 0) crystal axes. Because of this anistropy, B_l and B_t depend on the orientation of the layer planes. We assume here that the normal to the layer planes is in the (0, 0, 1) direction—this "cubic" orientation being the practical one for the (Ga, Al) As/GaAs layer materials. In converting (55) to (q, Q) variables, we replace $\lambda^2 + \mu^2$ by $\zeta^2 \equiv 1 - \nu^2$, the square of the "radial" direction cosine to the XY plane, and on averaging over the azimuthal directions of the XY plane we replace $\lambda^2\mu^2$ by $\zeta^4/8$. Then

$$A_l \to \frac{9}{2} \frac{q^2 Q^4}{(q^2 + Q^2)^3} \tag{56}$$

and

$$A_l + 2A_t \to \frac{8q^2Q^2 + Q^4}{2(q^2 + Q^2)^2}. \tag{57}$$

On substituting (56) and (57) in (53), we have

$$\begin{aligned} B_l &= 9/32, \\ 2B_t &= 13/32. \end{aligned} \tag{58}$$

Since acoustic-mode intraband scattering may be taken to be elastic,

$$Q^2 = 2(1 - \cos\theta)\, k^2, \tag{59}$$

where θ is the angle between initial and final $\mathbf{k}_\perp$ vectors, and k is their common length. The scattering rate is then

$$\frac{1}{\tau} = \frac{m^*}{\pi\hbar^3}\, \bar{S}_{II} \tag{60}$$

where the bar here means the average over θ. The mobility depends, however, on the rate with the scattering function weighted by $(1 - \cos\theta)$:

$$\frac{1}{\tau'} = \frac{m^*}{\pi\hbar^3}\, \overline{(1 - \cos\theta)\, S_{II}}. \tag{61}$$

The two-dimensional scattering function for the piezoelectric case, given by (54), is proportional to $1/Q$. The angle average in (61) then depends on

$$\overline{(k/Q)(1 - \cos\theta)} = \overline{\sin\tfrac{1}{2}\theta} = 2/\pi.$$

Then

$$\frac{k}{\tau'} = \frac{m^*}{\pi\hbar^3}\, \frac{2}{\pi}\, (QS_{II}) \tag{62}$$

with QS_{II} given by (54) and (58).

Collecting up these formulas, we find for the ratio of τ'_{piez} given by (54), (62) to τ_{def} given by (35):

$$\frac{k}{b}\, \frac{\tau_{\text{def}}}{\tau'_{\text{piez}}} = \frac{2}{\pi}\, [B_l + 2(s_l/s_t)^2\, B_t] \left(\frac{eh_{14}}{D}\right)^2. \tag{63}$$

The right-hand side of (63) is 2.74×10^{12} cm^{-2} for GaAs. Since τ_{def} is independent of E while τ'_{piez} is proportional to $E^{1/2}$ (where E here, and below, is the two-dimensional energy hitherto denoted by E_B, given by Eq. (3)), we have for the ratio of mobilities obtained with each scattering contribution

$$\frac{\mu_{\text{piez}}}{\mu_{\text{def}}} = \frac{3\sqrt{\pi}}{4}\, (\kappa T)^{1/2}\, \frac{\tau'_{\text{piez}}}{\tau_{\text{def}} E^{1/2}}. \tag{64}$$

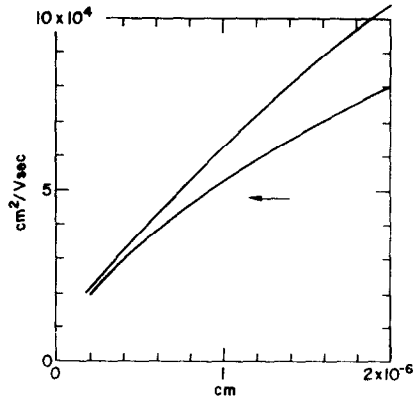

FIG. 3. Drift mobility versus layer thickness for electrons in a GaAs heterolayer, at $T = 150$ K. The upper curve is for polar scattering by optical-mode phonons and deformation-coupled scattering by acoustic-mode phonons. The lower curve includes a correction for piezoelectric-coupled acoustic-mode scattering. The arrow indicates the three-dimensional mobility.

Then for GaAs, on taking $b = a/3$ in (63), we find

$$\frac{\mu_{\text{piez}}}{\mu_{\text{def}}} = 1.79 \left(\frac{T}{100\text{ K}}\right)^{1/2} \frac{10^{-6}\text{ cm}}{a}. \tag{65}$$

As is illustrated by Matthiessen's Rule, the combined mobility tends to the smaller of the two separate mobilities.

Figure 3 shows the ohmic mobility for phonon scattering, versus layer width a, at $T = 150$ K. The upper curve is the mobility given by (35) and (48); the lower curve includes a correction for piezoelectric scattering, as calculated above, on the lines indicated in Section 4. (The arrow indicates, for comparison, the phonon-scattering mobility for the ordinary three-dimensional case, in GaAs at 150 K, calculated by Rode [8].) These ohmic mobility values are much greater than the experimental mobility values at 150 K, for modulation-doped material, reported by Dingle *et al.* [4].

4. MOBILITY

In the system considered here, where $\mathbf{l}$ the generalized mean free path is (approximated to be) parallel to $\mathbf{v}$ the electron velocity, the mobility is given by the relaxation time [9]

$$\tau' = l/v. \tag{66}$$

The ohmic drift mobility μ and Hall mobility μ^{H} are

$$\mu = (e/m^*)\langle \tau' E\rangle / \langle E\rangle \tag{67}$$

and

$$\mu^{\mathrm{H}} = (e/m^*)\langle(\tau')^2 E\rangle/\langle\tau' E\rangle, \tag{68}$$

where the angle brackets signify the thermal average. For two dimensions,

$$\langle F(E)\rangle \equiv \frac{1}{\kappa T}\int_0^\infty \exp\left(\frac{-E}{\kappa T}\right) F\, dE. \tag{69}$$

For deformation-coupled acoustic-mode scattering, τ' is equal to τ because the scattering is (near enough) isotropic. In two dimensions $\tau'(=\tau)$ is independent of energy E and consequently the mobilities μ_{II} and $\mu_{\mathrm{II}}{}^{H}$ are equal; but in three dimensions it is proportional to $E^{-1/2}$, and hence $\mu_{\mathrm{III}}{}^{H}/\mu_{\mathrm{III}}$ is equal to $\frac{1}{2}!\,\frac{3}{2}! = 3\pi/8$ and for Hall mobilities (37) has a different coefficient accordingly [10]. For piezoelectric-coupled scattering, in two dimensions, τ' is proportional to $E^{1/2}$ and hence μ/μ^{H} for this case is equal to $\frac{1}{2}(\frac{3}{2}!)^2 = 9\pi/32$, and the coefficient in (64) differs accordingly for Hall mobilities.

At low temperatures the phonon scattering consists of acoustic-mode scattering due to deformation coupling and to piezoelectric coupling. Since this scattering is virtually elastic, $1/\tau'$ is equal to the sum of the values it would have from each of the scattering contributions alone: $1/\tau_{\mathrm{def}}$ and $1/\tau'_{\mathrm{piez}}$ given by (35) and (63). Then

$$\mu = \int_0^\infty \exp(-u)[(\tfrac{3}{2}!/\mu_{\mathrm{piez}}) + (u^{1/2}/\mu_{\mathrm{def}})]^{-1}\, u^{3/2}\, du \tag{70}$$

(where u is $E/\kappa T$). With deformation scattering predominant, this is approximated by

$$\mu \simeq \mu_{\mathrm{def}}[1 - \tfrac{1}{2}!\,\tfrac{3}{2}!\,\mu_{\mathrm{def}}/\mu_{\mathrm{piez}})], \tag{71}$$

where the coefficient of the mobility ratio in the second term is $3\pi/8 = 1.178$. If, instead, $u^{1/2}$ in the denominator of the integrand, in (70), is replaced by the constant, $\frac{3}{2}!$, which makes the integral correct in the absence of any piezoelectric scattering, we obtain an instance of Matthiessen's Rule,

$$\mu \simeq \mu_{\mathrm{def}}\mu_{\mathrm{piez}}/(\mu_{\mathrm{def}} + \mu_{\mathrm{piez}}). \tag{72}$$

In the expansion of (72) corresponding to (71), the coefficient of the mobility ratio is one instead of the correct value $3\pi/8$. The lower curve in Fig. 3 gives the mobility calculated as $\mu_{\mathrm{def}}\mu_{\mathrm{piez}}/(\mu_{\mathrm{def}}+(3\pi/8)\,\mu_{\mathrm{piez}})$.

The treatment of polar optical-mode scattering is more complicated because the scattering is both anisotropic and inelastic. The J factor in (41), and hence the scattering function W_{II}, has in general a complicated dependence on E, θ and on the layer thickness. Scattering between sub-bands is involved, except for sufficiently narrow layers compared to $1/k_0$ and/or sufficiently low temperatures compared to T_0, as discussed in Section 3. The low temperature limit represented by Eq. (48) or Eq. (50) may be somewhat extended, and acoustic-mode

scattering included together with the optical-mode, in a treatment that amounts to expansion in powers of N_0, and should provide a realistic account of the lattice-scattering mobility at relatively low temperatures. This is developed in the following paragraphs.

Since the energy change in scattering is taken to be zero (acoustic mode) or $\pm E_0$ (optical mode) we have a ladder of equations, for $l(E)$, connecting l, v, etc., values at energies differing by a multiple of E_0. Let these be l_1, l_2,..., v_1, v_2,..., etc., where subscript i refers to E in the range $((i-1)E_0, iE_0)$. Then [9]

$$l_1 = \tau_1 v_1 + \beta_{12} l_2, \tag{73}$$

$$l_2 = \tau_2 v_2 + \beta_{21} l_1 + \beta_{23} l_3 \tag{74}$$

with the higher equations like (74), where β_{ij} is the average of $\cos\theta$, in the (i, j) scattering mode, multiplied by the relative frequency of that mode in the total rate $1/\tau_i$. The elastic (acoustic-mode) process is being taken to be wholly deformation-coupled, and hence isotropic. The critical truncating approximation is to drop the l_3 term from the solution of (73), (74) for l_1:

$$l_1 = (\tau_1 v_1 + \beta_{12}\tau_2 v_2 + \beta_{12}\beta_{23} l_3)/(1 - \beta_{12}\beta_{21}). \tag{75}$$

Then we substitute

$$\tau' = \tau_1 \frac{1 + (\tau_2 v_2/\tau_1 v_1)\,\beta_{12}}{1 - \beta_{12}\beta_{21}} \tag{76}$$

in (67) or (68), where the range of E in (69) can be formally taken as $(0, \infty)$ rather than $(0, E_0)$. Because β_{12} tends to zero like $E^{1/2}$, the second term in the numerator of (76) has a finite limit, proportional to the limit of β_{12}/v_1, at $E = 0$. We need to approximate (76) on the basis of the smallness of N_0 and of E/E_0.

Let the right-hand side of (48) be $N_0\nu_0$, defining the basic optical-mode scattering rate ν_0; and let ν_{ac} be the acoustic-mode rate, equal to $1/\tau$ where τ is given by (35). Then

$$1/\tau_1 = \nu_{ac} + N_0 K_{12}\nu_0, \tag{77}$$

$$1/\tau_2 = \nu_{ac} + ((N_0 + 1)\,K_{21} + N_0 K_{23})\,\nu_0, \tag{78}$$

$$\beta_{ij} = \binom{N_0}{N_0 + 1} K'_{ij}\nu_0\tau_i, \tag{79}$$

where

$$K_{ij} \equiv \overline{J_1(Q_{ij})}/J_1(k_0) \tag{80}$$

and

$$K'_{ij} \equiv \overline{J_1(Q_{ij})\cos\theta}/J_1(k_0). \tag{81}$$

The bar in (80), (81) means average over θ, as before. We have

$$K_{ji} = K_{ij}\,, \qquad K'_{ji} = K'_{ij}\,. \tag{82}$$

The expansions of K_{12}, K'_{12} in ascending powers of E begin

$$K_{12} = 1 + (\tfrac{3}{4}\gamma_1 + \tfrac{1}{4}\gamma_2)(E/E_0) + \cdots, \tag{83}$$

$$K'_{12} = -\tfrac{1}{2}\gamma_1(E/E_0)^{1/2} + \cdots, \tag{84}$$

where

$$\gamma_n \equiv \left(\frac{Q^n}{J_1}\frac{d^nJ_1}{dQ^n}\right)_{Q=k_0}. \tag{85}$$

We have to apply (83), (84) to three terms of (76). In the denominator,

$$\beta_{12}\beta_{21} \simeq (\tfrac{1}{2}\gamma_1)^2\, N_0(N_0+1)(\nu_0\tau_1)(\nu_0\tau_2)\, E/E_0\,. \tag{86}$$

In further estimating this quantity, we note that

$$\tau_1\nu_0 = (1 - \tau_1\nu_{ac})/N_0K_{12} \sim 1/N_0 \tag{87}$$

and

$$\frac{1}{\tau_2\nu_0} = K_{21} + N_0\left(\frac{K_{12}}{1-\tau_1\nu_{ac}} + K_{23}\right) \simeq 1. \tag{88}$$

Then (86) becomes

$$\beta_{12}\beta_{21} \simeq (\tfrac{1}{2}\gamma_1)^2\,(1 - \tau_1(0)\,\nu_{ac})\,E/E_0\,. \tag{89}$$

We have found in Section 3 that the acoustic and optical terms of $1/\tau_1$ should be comparable in a temperature range that normally lies near 100 K; the value of the middle factor of (89) will be $\lesssim 1$ accordingly. Since $-\gamma_1$ will lie between 1 and 2, a typical value of the coefficient of E/E_0 in (89) should be somewhat less than one. Similarly

$$\tau_1(E)/\tau_1(0) = 1 - (\tfrac{3}{4}\gamma_1 + \tfrac{1}{4}\gamma_2)(1 - \tau_1(0)\,\nu_{ac})(E/E_0) + \cdots \tag{90}$$

Again, the coefficient of E/E_0 is ~ 1. For the β_{12} term of (76), we have

$$(\tau_2v_2/\tau_1v_1)\,\beta_{12} \simeq -\tfrac{1}{2}\gamma_1N_0\nu_0\tau_2\,.$$

Then by (88)

$$(\tau_2v_2/\tau_1v_1)\,\beta_{12} \simeq (-\tfrac{1}{2}\gamma_1)\,N_0\,. \tag{91}$$

On substituting from (89), (90) and (91) in (76), we can obtain an estimate for the lattice-scattering mobility at relatively low temperatures where N_0 is small, and

optical-mode scattering and deformation-coupled acoustic mode scattering are both appreciable but piezoelectric-coupled is not:

$$\mu \simeq \frac{e}{m^*}\tau(0)\left(1-\frac{1}{2}\gamma_1 N_0\right)\left[1+\frac{1}{2}(\gamma_1{}^2-3\gamma_1-\gamma_2)(1-\tau(0)\,\nu_{ac})\frac{T}{T_0}+O\left(\frac{T}{T_0}\right)^2\right] \tag{92}$$

where $\tau(0)$ is the same as $\tau_1(0)$.

In general we have a more complicated situation. For optical-mode scattering within a subband, the product of maximum and minimum Q values, for given initial and final k values, is $k_0{}^2$; hence Q ranges from $\ll k_0$ to $\gg k_0$ when the initial or final k is not $\ll k_0$. We also have to consider scattering between subbands, and want to calculate hot-electron as well as ohmic transport properties. It seems clear, therefore, that we need to pass from analytic solution of the Boltzmann equation to Monte Carlo methods [11]. The following section discusses the application of Monte Carlo to the scheme developed in Section 3; but actual Monte Carlo computations are not reported in the present paper.

5. Monte Carlo Calculations

Suppose that our model electron system consists of the first n subbands, with their itinerant states represented by the energy scheme (8). For an electron in a given subband, the scattering processes are in one of n possible categories: to a final state in the same subband or to a final state in any one of the $(n-1)$ others. For each of these, we have the three lattice-scattering possibilities of acoustic-mode (taking absorption and emission of the phonon together) and optical-mode absorption or emission. The maximum number of scattering "channels" is then $3n$. If an upper bound can be established for the scattering rate in each channel (as we shall in fact do, below), say λ_i for the ith, then we have a maximum total rate $\Gamma = \sum_i \lambda_i$ which can be used in the now standard procedure to generate the "paths" between scatterings, with durations s having the distribution function

$$\Gamma \exp(-s\Gamma). \tag{93}$$

Computer-generated random numbers are then used to assign a given scattering to one of the possible channels or to a "self-scattering" (representing the difference between Γ and the actual total scattering rate out of the particular initial state), and to a specific final state for the selected channel, with the correct relative frequencies.

Of course, for a large part of the range of the energy E of the initial state in scattering, the number of active scattering channels will be less than $3n$ and for these $\sum\lambda$ will have some value, Γ', less than Γ. The difference corresponds to a contribution $(\Gamma-\Gamma')/\Gamma$ to the self-scattering probability, which is just a step function of E since $\Gamma'(E)$ is a step function. Whether a given scattering, out of the total rate Γ, is one of this category of self-scatterings should be the first alternative decided, in the Monte

Carlo scattering algorithm; the contribution of these events to the total computer time, in simulating a particle "history" of given length, will then be small.

For polar optical-mode scattering, upper bounds of the scattering rates are easily found. Since, if k_1 and k_2 are the initial and final wavevector lengths,

$$Q^2 = k_1^2 + k_2^2 - 2k_1k_1 \cos\theta \tag{94}$$

we have for intraband scattering

$$\overline{\left(\frac{1}{Q^2}\right)} = \frac{1}{|k_1^2 - k_2^2|} = \frac{1}{k_0^2}. \tag{95}$$

Therefore, since the right-hand side of (44) is the upper bound of the left side, the intraband rates are less than

$$\lambda_{n,\pm}^{\text{opt}} = \left(N_0 + \frac{1}{2} \pm \frac{1}{2}\right) \frac{\pi}{2b_n} \frac{e^2}{\hbar} \left(\frac{1}{\epsilon_\infty} - \frac{1}{\epsilon_0}\right). \tag{96}$$

For the interband scattering we take the maximum rates as given by $J_{mn}(0)$. Then for the case of Eq. (7) they are, by the second of Eqs. (43),

$$\lambda_{mn,\pm}^{\text{opt}} = \left(N_0 + \frac{1}{2} \pm \frac{1}{2}\right) \frac{ak_0^2}{\pi} \frac{e^2}{\hbar} \left(\frac{1}{\epsilon_\infty} - \frac{1}{\epsilon_0}\right) \frac{m^2 + n^2}{(m^2 - n^2)^2}. \tag{97}$$

For a total of n bands, the upper bound of the optical-mode interband rate for scattering from the mth band will be obtained by replacing the final factor of (97) by the sum

$$L_{mn} = \sum_{l=1}^{n} (l \neq m) \frac{m^2 + l^2}{(m^2 - l^2)^2}. \tag{98}$$

The contribution to Γ will then be given by the maximum of L_{mn} with respect to m.

For those scatterings in which one of these optical-mode channels was selected, the Monte Carlo scattering procedure could be completed as follows. For given k_1, k_2 (i.e., for given initial energy E, and channel) the scattering rate is actually proportional to

$$\bar{J}_* = (1/\pi) \int_0^\pi J_*(Q)\, d\theta \tag{99}$$

where Q is given by (94). Then the event should be taken to be a physical scattering if

$$\bar{J}_n > (\pi/b_n k_0^2)\, R$$

or (100)

$$\bar{J}_{mn} > J_{mn}(0)\, R$$

(for an intraband or an interband process respectively) where R is the usual random number from a population uniformly distributed in (0, 1); else it is to be yet another "self scattering." For a physical scattering, a scattering angle θ may then be found by (a) generating an angle $\theta = \pi R$ belonging to a uniform distibution in $(0, \pi)$, and hence a value of Q by (94) [12]; (b) applying

$$J_*(Q) > J_*(|\, k_1 - k_2 \,|)\, R \tag{101}$$

as the condition for accepting this scattering angle as the actual one for the scattering event; (c) if (101) is not satisfied, repeating (a–c). In implementing the foregoing, the $\bar{J}_*$ could be tabulated as a function of E and the J_* tabulated as a function of Q^2, in the initialization phase of the computation(s), and values obtained by a "look up" procedure during the actual Monte Carlo simulation.

For the acoustic-mode scattering, so long as the piezoelectric contribution is disregarded, nothing so complicated is required. The scattering is isotropic and the rate for each channel is independent of E. Then the contributions to Γ, corresponding to (96) and (97), are just the $1/\tau$ given by (35) with either intraband or interband b value. When a particular acoustic-mode channel is selected, the scattering angle is to be a member of a uniform distribution in $(0, \pi)$—or, equivalently, a final-state angle can be chosen from a uniform distribution. As we have seen, however, the piezoelectric-coupled scattering may not necessarily be neglected. For hot electron conditions in particular, we accordingly need at least a means of estimating, and possibly of accurately calculating, its effect. The remainder of the present section concerns the unusual problems that this entails. For piezoelectric-coupled (intraband) scattering, the quantity given by (60) is infinite—the integral of the scattering function $W_{\text{II}}(\ ,\ )$ over final states diverges [13]. The scattering rate of change of f

$$\int [f(\mathbf{k}')\, W_{\text{II}}(\mathbf{k}', \mathbf{k}) - f(\mathbf{k})\, W_{\text{II}}(\mathbf{k}, \mathbf{k}')]\, d^2\mathbf{k}' = Gf \tag{102}$$

is finite, but the inscattering and outscattering parts (given by the first and second terms of (102), respectively) are not separately finite in the present case. The finiteness of the combination, corresponding to the finiteness of (61), comes from the vanishing of $f(\mathbf{k}') - f(\mathbf{k})$ as $\mathbf{Q} = \mathbf{k}' - \mathbf{k}$ tends to zero [14].

The Boltzmann equation

$$\mathbf{F} \cdot (\partial/\partial \mathbf{p}) f = Gf \tag{103}$$

(where $\mathbf{F}$ is the force on a carrier particle due to the electric field, or electric and magnetic fields, and $\mathbf{p}$ is $\hbar\mathbf{k}$) can normally be written

$$\left[\frac{1}{\tau} + \mathbf{F} \cdot \frac{\partial}{\partial \mathbf{p}}\right] f = \Omega f, \tag{104}$$

where the integral operator Ω is the inscattering part of the scattering operator G, giving the first term of (102), and hence as

$$f = \Pi \Omega f, \tag{105}$$

where the integral operator Π, the inverse of [ ] on the left of (104), is the "path" operator transforming the distribution of states after the scatterings into the distribution of states preceding the scatterings [15]. The form (105) represents the computational method developed especially by Rees, in which scattering and path operators are applied alternately to a grid-based numerical representation of f, and a solution generated by iteration; and it also corresponds to the Monte Carlo procedures, in which a stochastic sequence of particle variables is generated by alternating scattering and path events.

When intraband acoustic-mode piezoelectric-coupled scattering is to be taken into account, we can separate W, and hence G, into a nonpiezoelectric part and a piezoelectric part, to be denoted here by subscripts "0" and "1", respectively. Then (104) may be replaced by

$$\left[\frac{1}{\tau_0} + \mathbf{F} \cdot \frac{\partial}{\partial \mathbf{p}}\right] f = \Omega_0 f + G_1 f \tag{106}$$

and (105) by

$$f = \Pi_0 \Omega_0 f + \Pi_0 G_1 f. \tag{107}$$

One would expect to be able to compute the right-hand side of this equation for a grid-based numerical representation of f and hence proceed in the same manner as for (105). To implement (107) by Monte Carlo simulation, however, it is evident that we must elaborate the usual procedures [11] in two ways, to take account of the singular and nonpositive nature of individual "scattering functions" on its right-hand side:

(a) The three terms of (107), consisting of the inscattering given by Ω_0 and the inscattering and outscattering parts of G_1, should be represented by three alternative channels for the scattering event. For both the second and the third of these the scattering angle is to be generated as a random variable, and a numerical value for the scattering probability (i.e., for S_{II}) obtained for the actual selected angle (the Q value).

(b) A weight, w, should be included, together with $\mathbf{k}$ and the band index, in the set of particle variables; it will be constant along the path trajectories, but in general be changed in scattering events. The weight variable (which can be initialized $w = 1$) will accommodate both the $1/Q$ singularity of W_{II} and the negative sign proper to the outscattering term. It is, of course, to be included in the estimators for computing expectations or distributions from the sequence of states generated in the Monte Carlo simulation.

An appropriate weighting function $P(\ ,\ )$ can be separated out of the scattering function: i.e.,

$$W(1, 2) = P(1, 2)\, \tilde{W}(1, 2), \tag{108}$$

where the quotient $\tilde{W}(\ ,\ )$ does not have the singularity and is to be used in place of $W(\ ,\ )$. In a transition $1 \to 2$, the particle weight is multiplied by $P(1, 2)$, and by

another factor to be specified below. For a transition representing the outscattering term of G_1, the P value would be taken negative and w would change sign. In the choice between the three channels representing the right-hand side of (107), an arbitrary channel weight $z < 1$ can be assigned to the first and weights $\frac{1}{2}(1 - z)$ accordingly to the second and to the third. (One may regard $(1 - z)/z$ as the frequency with which the piezoelectric scattering process is "sampled" in generating the distribution of particle states.) Then the ratio of final w value to initial w value in a scattering is to be $1/z$ for the Ω_0 term of (107) and $(\pm)P\tau_0/(\tilde{\tau}\ \frac{1}{2}(1 - z))$ for the G_1 terms. If we take for $\tilde{W}$ the acoustic-mode deformation-coupled scattering function, then

$$P = \frac{S_{\text{piez}}}{S_{\text{def}}} = \left(\frac{eh_{14}}{D}\right)^2 \left(B_l + 2\left(\frac{s_l}{s_t}\right)^2 B_t\right) \frac{b}{Q} \tag{109}$$

and $\tilde{\tau}$ is τ_{def}.

The interband piezoelectric-coupled scattering is evidently small and could, if taken into account, be handled in a way similar to that of the polar optical scattering above. It is not investigated here.

6. Discussion

Phonon scattering of electrons in a two-dimensional "heterolayer" system—in particular for a layer of the polar semiconductor GaAs—has been analyzed. It was found to be complicated, and to result in a two-dimensional electron transport system which may be treated theoretically by specially adapted computer methods. Even so, the scattering theory developed above is incomplete in scope and idealized in assumptions.

1. Equation (7)—in conjunction with Eqs. (1), (2), and (4)—does not adequately describe the electron wavefunctions. This has been discussed in Footnote [5]. In addition, the states with quantization energy near the band edge for the barrier material, and in the itinerant range above it, need further consideration.

2. The lattice modes of the scattering phonons have been assumed to be those of the homogeneous layer material (specifically, bulk GaAs). The modification due to the well-and-barrier layer structure, and the possible contribution of phonon modes associated with the interfaces themselves, has not been discussed here. (An "electrostatic" addition to the effective deformation potential, from the coulomb interaction of electrons in the well layers with donor ions in the barrier layers, will be numerically significant only at the highest doping levels.)

3. A screening of the electric field of the polar lattice modes, peculiar to this system and due to the polarizability of the quantized electron states in the x direction (normal to the layer plane), may be important at electron concentrations of interest.

4. We have assumed the electron systems of the "well" layers (when we in fact have more than one, as in a superlattice) to be independent; but there are possible

interactions between them. A possible mode of interaction is the "hybridization" effect of the overlap interaction between the states of neighboring layers which gives the superlattice band width. There could also be a phonon drag effect from phonons emitted in an electron scattering in one layer and absorbed in scattering in another layer, and similarly the currents in neighboring layers could interact by mutual coulomb scattering of their electrons.

A normally important mode of scattering, in the materials considered here, is coulomb scattering by donor and acceptor ions, also a more complicated phenomenon than in homogeneous semiconductors [16, 17]. Another kind of scattering, which a sufficiently complete analysis of the two-dimensional electron transport properties might need to include, is that due to "roughness" of the interfaces [17].

A large, and somewhat repetitive, journal literature exists on the analogous phenomenon of two-dimensional electron transport for the inversion layer in Si at an interface with silicon oxide. This differs from the system considered here especially in that the electron states differ (on account of the inversion-layer field), silicon is nonpolar, and the silicon conduction band has a many-valley band edge with anisotropic minima. There is much less published work on the system considered here. Ferry [18] gives a result for polar optical-mode scattering which evidently is equivalent to the case of Eqs. (44), (96) above. Hess [16] gives a formula for the acoustic-mode scattering rate which is one half of the present result, from Eq. (35), for the deformation-coupled. rate. (The former may represent emission or absorption alone, therefore.) From the work of the present paper, it appears that phenomena of interest are not correctly described by conveniently simple formulas except in some special cases.

Reduction of the ion density to the level where it does not significantly affect transport properties would be desirable not only for device applications, but also to further investigation of the physics of these heterolayer systems, by isolating the phonon scattering for study. Although this lattice-mode scattering alone, for polar-semiconductor heterolayers, evidently requires numerical calculation by computer, possibly using pretabulated functions, for analysis of electronic transport properties of interest, there are more parameters that it depends on, and that might be deliberately varied in experimental investigations, than in ordinary homogeneous material. One can, obviously, vary the layer width. It may also be feasible to vary the density of the initerant electrons (per unit area of a heterolayer) virtually independently of other quantities, providing a means of experimental study of the effects of electron degeneracy and of screening by the itinerant electrons as mentioned above. Consequences of various alloy profiles in a layer — not just a constant concentration — would be of interest. Interaction between currents in neighboring layers could be another subject for experimental and theoretical study. This incomplete list will help to indicate that the physics of the semiconductor "mesostructures" that one can expect to be provided by MBE growth techniques should be rich in new and interesting features.

Note added in proof. An investigation of the effects of screening (*J. Vac. Sci. Tech.*, in press) shows that for phonon scattering these normally are important only at high electron concentrations. It is also found that the effects mentioned as point 3 above, "secondary screening," are not normally important.

References and Footnotes

1. L. Esaki and L. L. Chang, *Thin Solid Films* **36** (1976), 285.
2. L. Esaki and L. L. Chang, *Phys. Rev. Lett.* **33** (1974), 495.
3. R. Dingle, *Festkörperprobleme* **15** (1975), 21.
4. R. Dingle, H. L. Störmer, A. C. Gossard, and W. Wiegmann, *Appl. Phys. Lett.* **33** (1978), 665.
5. Even assuming perfect layers of the two crystals alternating at perfect interfaces, with no macroscopic fields superposed, (7) and (8) are not quite correct. The true coefficient of x in (7) is somewhat smaller than given here, as though a exceeded the layer width by an amount $\sim$ the lattice constant, (a) because the energy step (work function difference) from well layer to barrier layer is not in general very large compared to the E_n, (b) because the correct boundary condition at the interface is not continuousness of the envelope function Ψ. The E_n consequently will be somewhat less than the values given by (8). (The amplitude of Ψ in the barrier layers, for the well levels, will be substantially smaller than it would be if Ψ were continuous, which justifies including only the well-layer part of Ψ in the matrix elements for electron–phonon coupling.) In addition for relatively large layer widths and doping levels the electrostatic field at the interfaces and associated "hump potential" in the well layers will not be small enough to be safely neglected. The idealization (7), (8) is appropriate to the purposes of the present investigation.
6. See, for example, J. M. Ziman, "Electrons and Phonons," Chap. 10, Oxford Univ. Press, London/New York, 1960.
7. J. D. Zook, *Phys. Rev. A* **136** (1964), 869.
8. D. L. Rode, *Phys. Rev. B* **2** (1970), 1012.
9. For the generalized mean free path used here and its calculation, and the application to the Hall effect, see: P. J. Price, *IBM J.* **1** (1957), 239, especially Section 5; *IBM J.* **2** (1958), 200; *Phys. Rev. B* **6** (1972), 4882.
10. For the composite conductivity from two or more subbands, however, the mobility ratio can deviate substantially from the values for the individual subbands.
11. For the methods and terminology, in Monte Carlo calculation, assumed here, see: P. J. Price, Chapter 4, *in* "Semiconductors and Semimetals" (R. K. Willardson and A. C. Beer, Eds.), Vol. 14, Academic Press, New York, 1979.
12. A Monte Carlo algorithm entailing only a few arithmetic operations (in addition to generation of random numbers) exists for supplying the appropriately distributed $\cos\theta$ values directly. The value of $\sin\theta$ would then be required, for the present purpose, but only for the "successful" $\cos\theta$ values satisfying (101).
13. This is literally true for S_{II} proportional to $1/Q$ as in (54). Although screening, "polaron" effects, etc., may remove the singularity in S_{II} and hence make the scattering rate (60) finite, we need to determine the consequences of the $1/Q$ dependence. In any case the behavior represented by the $1/k$ dependence of τ', the unbounded increase of the scattering rate of change of f with decreasing E, will effectively remain and will preclude conventional Monte Carlo procedures.
14. There is an analogous situation for the ordinary three-dimensional case, as pointed out by Rode (Ref. [8]).
15. When the total scattering rate (usually denoted by Γ when it is constant) is not constant, some care may be needed in the correct use of factors τ and $1/\tau$ in these formulas. See: P. J. Price, *IBM J.* **14** (1970), 12.
16. K. Hess, *Appl. Phys. Lett.* **35** (1979), 484.
17. S. Mori and T. Ando, *J. Phys. Soc. Japan* **48** (1980), 865.
18. D. K. Ferry, *Surf. Sci.* **75** (1978), 86.